2022

Chemical Analysis of Amoxicillin Samples Using Ultra Performance Liquid Chromatography in Tandem with Mass Spectrometry for the Distributed Pharmaceutical Analysis Laboratory

Sophie Samiee
Pitzer College

Chemical Analysis of Amoxicillin Samples Using Ultra Performance Liquid Chromatography in Tandem with Mass Spectrometry for the Distributed Pharmaceutical Analysis Laboratory

A Thesis Presented

By

Sophie Samiee

To the Keck Science Department

Of Claremont McKenna, Pitzer, and Scripps Colleges

In partial fulfillment of

The degree of Bachelor of Arts

Senior Thesis in Biology

2022

Table of Contents

Abstract

The global health crisis of "fake" drugs is rampant worldwide and causes 1 million deaths and $30 billion in damage annually, according to a recent report by the United States Pharmacopeia in 2021. Substandard and falsified medicines remain uncontrolled due to underreporting, poor detection methods, and a lack of cooperation between countries. To combat this, the University of Notre Dame and Chemists Without Borders established the Distributed Pharmaceutical Analysis Laboratory (DPAL) in 2014 to provide high quality, validated analysis of pharmaceutical samples from partners in the developing world. Heretofore, ultra-performance liquid chromatography in tandem with mass spectrometry (UPLC-MS) has not been utilized by DPAL institutions. This research presents an effective methodology for analyzing amoxicillin samples using UPLC-MS.

Introduction

Drug Counterfeiting:

Substandard and falsified (SF) medical products are a prominent global health threat that has detrimental health, economic, and socioeconomic impacts. Despite regulatory agencies' efforts to minimize the distribution of SF medical products, such products are found worldwide on a scale that results in one million deaths and $30 billion in damage annually.[1] To counteract this, more extensive testing of medicines has to be implemented to decrease the circulation and consumption of SF medical products.

Substandard medical products are defined by the World Health Organization (WHO) as "authorized medical products that fail to meet quality standards, specifications, or both."[2] Expired ingredients or improperly manufactured, shipped, or stored goods can all result in a substandard medical product that may inflict harm on consumers. In contrast, falsified medical products are *deliberately* and *fraudulently* misrepresented.[2] To pose as the true product, falsified medical products are often disguised in packaging that is identical to the that of the true product, requiring testing to confirm the contents (Figure 1).[3] Furthermore, falsifiers target both lifesaving and lifestyle medications, generic and branded, which allows for ample avenues of falsification.[4] Both substandard and falsified products may contain no or an incorrect level of an active pharmaceutical ingredient (API), or could also contain other substances that are unsuitable for consumption such as benign powders or toxic compounds.[4] Contamination of medicines with toxic compounds is more fatal than that of benign contaminants—most commonly corn and potato starch, pollen, and chalk—since patients are not only receiving incorrect levels of API, but also ingesting noxious substances.[5]

Figure 1. An example of a falsified drug and its packaging (left) compared to a true medical product (right).[7]

Some SF medical products that contain no or an incorrect level of API seek to feign treatment by masking symptoms associated with illness. In 2005, a 23-year-old was treated in a Burmese hospital for malaria, but unknowingly received falsified artesunate—a first-line drug for treatment of malaria—that contained acetaminophen as its main API.[5,6] Since this, acetaminophen has been repeatedly reported APIs in antimalarials, likely due to its pain relieving and fever reducing abilities. [5]

SF medical products can also contain a variety of toxic compounds. For instance, in 2006 a Chinese manufacturer sold diethylene glycol—the active ingredient in antifreeze—as pharmaceutical grade glycerin.[5] More than 60,000 bottles of cough syrup were contaminated which resulted in 219 Panamanian deaths from acute kidney failure; however, this is likely an underestimation of mortality due to difficulties tracking distribution.[5] A similar contamination of diethylene glycol in teething syrup resulted in 84 Nigerian deaths between November 2008 and February 2009.[5] Years later in 2011, the Chinese State Food and Drug Administration found that 13% of capsule manufacturers were making drugs that contained unsafe levels of chromium—a toxic metal—and that 254 companies were the sources of these tainted medicines.[5]

The impacts of SF medical products are multifaceted (Figure 2). SF medical products can have negative health consequences, such as lack of efficacy that results in worsened disease symptoms or toxicity from incorrect ingredients (Figure 2). Further, the failure to cure or prevent a disease can increase mortality, morbidity, the prevalence of disease, and in some cases, increase the progression of antibiotic resistance.[2] As a result, patients may experience a loss of confidence in health care professionals, programs, and institutions, thereby decreasing their likelihood to reach out to licensed professionals in the future (Figure 2).[2]

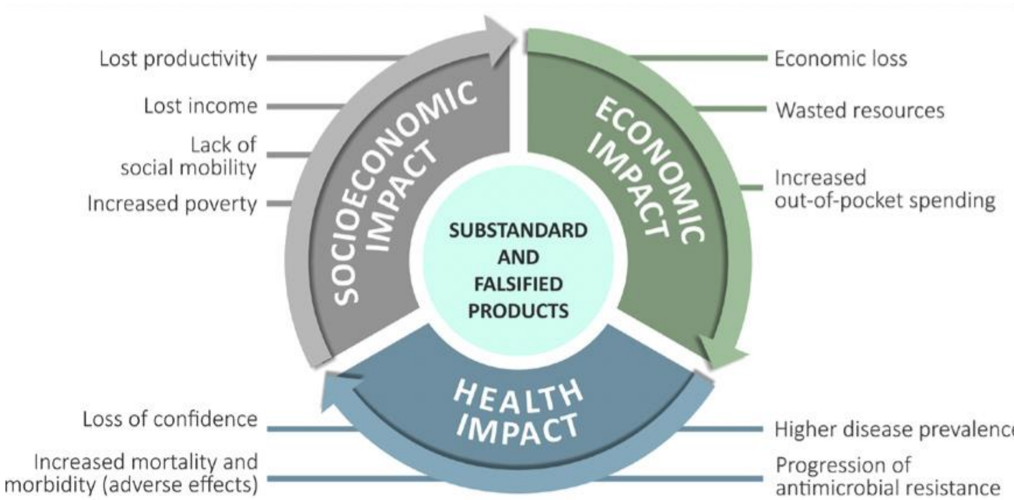

Figure 2. Multifaceted impacts of SF medical products.[2]

In addition, the economic and socioeconomic impacts of SF medical products can also be severe. Patients, families, healthcare systems, and manufacturers can all suffer extreme economic hardships from SF medical products (Figure 2).[2] The increased strain on medical resources, staff, and infrastructure, burdens health care professionals, medicine regulatory agencies, and law enforcement.[2] Prolonged illness or mortality due to SF medical products result in lost income and household productivity levels. However, it can be difficult to quantify the social costs of SF medical products such as the impact on gross national income, life expectancy, level of employment, social mobility, and how trust is negotiated between patients and health care systems, all of which can trap patients into a cycle of poor health and poverty.[2] These multifaceted impacts of SF medical products can stunt economic and social development and growth. Additionally, these consequences are amplified with the rise of online health care and drugstore options that readily elude regulation and pose a greater risk on fraudulent distribution practices.[4]

Globalization of Drug Distribution:

The increased globalization of medical product distribution has also given rise to more SF medical products (Figure 3). The lack of consensus regarding the specific definitions of SF medical products lead to an underreporting of SF products, further inhibiting efforts to determine high-risk medications, geographical regions, and vulnerable patient populations that have greater potential of exposure to SF medical products.[3]

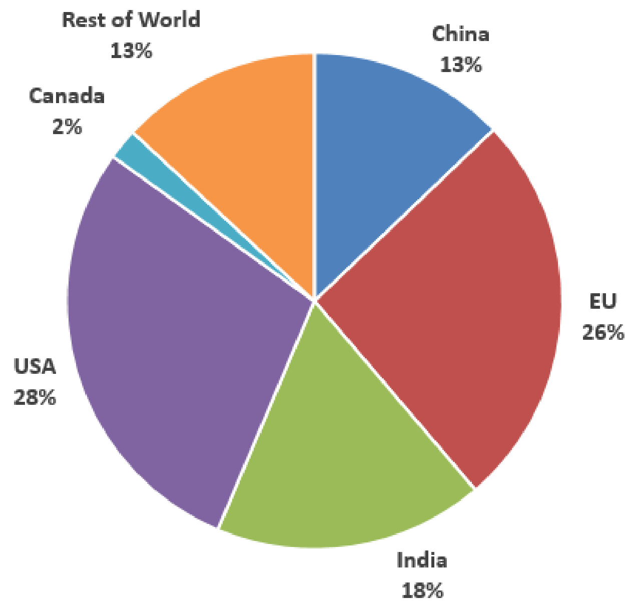

Figure 3. Percentage of API manufacturing sites by country or region as of 2019.[8] Factors resulting in increased globalization of API manufacturing include: availability of low-cost labor, fewer environmental regulations regarding buying, handling and disposing of toxic chemicals, and a shift in US interest towards drug discovery and development.[8]

Legal regulations and penalties regarding health products also lack consensus across countries, resulting in ambiguous regulatory policies across borders.[2,4] For instance, Rwanda successfully reduced the prevalence of falsified medical products that target tuberculosis and malaria treatment by prohibiting private sales of therapies; however, their neighboring countries have not implemented similar strategies, impeding the effectiveness of these policies.[3] To address this, Rwanda is now advocating for the redefinition of generic and falsified medications, which was followed by the development of a regional law in East Africa banning falsified medicines. Rwanda is thereby illustrating two major political actions that need to be enacted to globally tackle the SF medical product health threat: 1) the requirement of a global definition of SF medical products, and 2) the explicit ban of all SF medical products. In fact, as a step towards introducing standardized definitions to combat SF medical products, the World Health Assembly recently introduced new definitions of substandard, spurious, falsely-labeled, falsified, and counterfeit medical products.[3]

Factors that can Increase the Prevalence of SF:

Among patients, some are more vulnerable to SF medical products and their distributors than others. Research indicates that the prevalence of SF medical products is closely tied with socioeconomics, as around 11% of medicines worldwide are SF, yet this percentage tends to be greater in low- and middle-income countries (LMICs); this discrepancy between countries results in a greater economic burden of SF medical products in LMICs (Figure 4).[2,9]

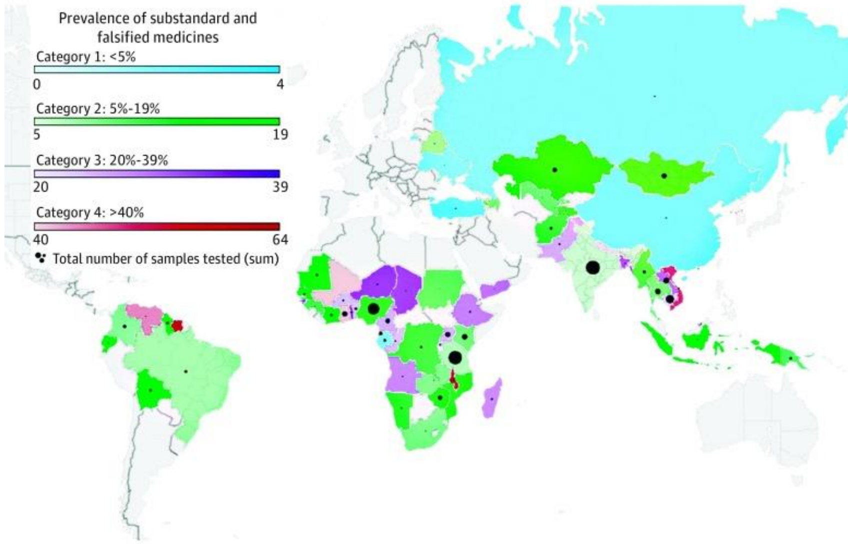

Figure 4. Reported national prevalence of SF medicines based on results from a meta-analysis study in 2008. Each country is represented as a black circle with the diameter of the circle increasing proportionally to the samples tested. Prevalence is delineated by color and by gradation, with a darker color representing a higher prevalence.[9]

In addition, the types of medical products that tend to be SF differ by socioeconomic status. The most commonly reported SF medical products in high-income countries (HICs) are hormones, steroids, and supplements, while the most reported SF medical products in LMICs are antimalarials and antibiotics for treating malaria, TB, HIV, and AIDS.[3] Between 2013 and 2017, 42% of reported SF medical products were from Africa, with antibiotics and antimalarials representing around 36% of falsified products.[3] This, in turn increases the rate of antimicrobial resistance due to incorrect dosages, allowing for bacterial proliferation and spread in already strained communities (Figure 4).[9]

During times of shortages, SF medical products flourish due to consumers' increased vulnerability. This was most recently observed during the COVID-19 pandemic. In Mexico, the Federal Commission for the Protection against Sanitary Risks issued a health alert about the falsification and illegal marketing of drugs claiming to prevent and cure COVID-19.[10] Around 33 million SF face masks, tests, and diagnostic tests; 8 tons of raw materials, chemicals, and antivirals;

and 70,000 liters of sanitizers were seized in Europe.[10] During the first five months of 2020, reporting of SF medical products in Brazil was four times higher than all of 2019.[10] This pattern of increased prevalence of SF medical products was seen throughout the pandemic, rendering global supply chains vulnerable to the entry and distribution of SF health products.[10] Due to this amplified vulnerability, it has become increasingly crucial to develop and instigate solutions to attack the drug counterfeit issue.

Strategies to Decrease Distribution of SF Drugs:

Efforts to help eliminate the entry of SF medicines into the supply chain have not only included standardizing the definitions and legal regulations of SF medical products. The establishment of the Falsified Medicines Directives (FMD) in the EU represents an important step in the battle against SF products.[3] In 2019, the FMD sought to require all medicines sold in EU to have tamper-evident features and scan codes to update the National Medicines Verification System about the drug's status along the supply chain.[3] In addition, the FMD's mission emphasizes the education of pharmacy professionals on SF medical products so that they may, in turn, educate patients.[3]

A survey administered to 200 Swedish physicians further emphasized the need to increase the awareness of illegal and falsified medicines and reporting procedures among both physicians and patients.[4] Among the surveyors, 21% had never heard about SF medical products; 88% had faced a problem with SF medical products; 56% did not warn patients about SF medical products; and 67% did not know how to report suspicious medicine.[4] Given this lack of awareness, it is not surprising that patients often do not realize if they have consumed SF medical products and more readily assume that they are simply not responding well to the treatment.[3] This leads to continued distribution of these products and emphasizes the demand for increased education and reporting accessibility.

Further efforts to decrease the prevalence of SF medical products were suggested in response to COVID-19. Suggestions include increasing pressure on local regulatory authorities to identify gaps in their medical product distribution systems and capabilities.[10] Further, handbooks containing strategies for handing sensitive medicines that are specific to local requirements and conditions could decrease the prevalence of substandard medicines.[10] Expensive, analytical assays for testing and releasing products into the supply chain have also been suggested as a method for preventing falsified products' distribution.[10] Assays can provide an accurate and comprehensive record of a sample's ingredients and component concentrations, offering an effective means of testing for both substandard and falsified medical products.

To increase the analytical assaying of medicines, while mitigating the costs, the Distributed Pharmaceutical Analysis Laboratory (DPAL) was established at Notre Dame in partnership with Chemists Without Borders. DPAL is a collaboration between academic institutions around the world with the goal of determining the quality of medicines collected from partner organizations in LMICs, who often do not have the resources to carry out expensive assays, yet are most vulnerable to SF medical products.[11] DPAL takes advantage of higher-education institutions' access to equipment and students driven to learn and execute assays, invaluable tools that allow for the otherwise inaccessible analyses of medicines from Kenya, Uganda, Tanzania, India, Nepal, and Malawi. Using different assay techniques, pharmaceutical alerts can be made upon identifying suspicious samples to help decrease potential detrimental effects of SF medical products.

Assays Used to Identifying SF Medicines:

Assay techniques differ in what characteristics of a sample they can report on. The general technique of liquid chromatography (LC) has been highly utilized to carry out pharmacopeia assays among DPAL institutions due to its ability to isolate components of a mixture.[11,12] Compounds that absorb light can be isolated using ultraviolet-visible spectroscopy (UV-vis) based on their retention times—amount of time for the solute to pass through the column—which is dependent on the compounds' affinity to and interactions with the silica and solvent, stationary and mobile phases respectively (Figure 5).[12,13] LC can also report the concentration of analyte based on the detector's response and the resulting chromatographic peak integrities.[14] To identify the isolated components in a column, the retention times of the constituents are compared to those of known samples (Figure 5).[12] Thus, LC can be instrumental in identifying SF medicines and monitoring the quality of medicines in clinical settings. For instance, a medicine can be both safe and accurate when it first arrives in a hospital or other clinical setting but undergo degradation once there. A 2019 study utilized HPLC to investigate the stability of intravenous amoxicillin under different conditions and time points.[15] This allowed for the ensured efficacy and safety of administered drugs over long periods of time and is a prime example of the pharmacological information that can be derived from LC.

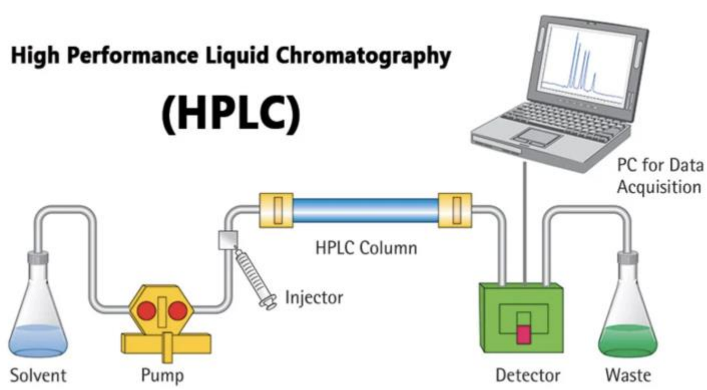

Figure 5. Depiction of HPLC.[16] The strength of the pump controls the pressures achieved in the column.

Advancements to LC have been made, such as high-performance liquid chromatography (HPLC) and ultra-performance liquid chromatography (UPLC), which differ in speed, resolution, and sensitivity (Figure 5).[17] LC columns travel only by the force of gravity, while HPLC and UPLC have increasingly greater pressures, allowing for faster run times, enhanced resolutions even with smaller particle sizes, and better peak separation due to greater column pressures.[12] LC assays require purified solvents, analytical-grade balances and glassware, columns, and pharmaceutical standards, which render them expensive and scarcely available in LMICs. DPAL takes advantage of LC's accessibility in HICs and higher-education institutions and has developed a handbook to provide standard operating procedures (SOPs) for carrying out pharmaceutical assays via HPLC to enable participation of member institutions.[18]

Once system suitability is established for a given drug, a DPAL collaborator can then begin sample analysis. Over 1,200 samples have been analyzed, and 168 have failed HPLC assay, including falsified acetaminophen tablets, degraded injectable ceftriaxone, and expired amoxicillin/clavulanate (Figure 6).[11] This highlights the impact of DPAL on pharmaceutical standards and safety on a global scale.

Figure 6. A substandard batch of amoxicillin/clavulanate, Dafraclav 625, from Eldoret, Kenya whose contents were found to be expired. Soon thereafter, the manufacturer was notified and the lot number was flagged.[11]

Though demonstrated as a useful tool in pharmacopeia identification, LC in DPAL's SOP requires an external standard every 4 runs to ensure the values of integrated intensities for the external standard fall within 2% relative standard deviation (RSD) to ensure accuracy and range of the instrument being used.[18] Additionally, LC is limited by UV-active compounds. Though LC on its own can indicate the purity of pharmaceuticals, LC in tandem with mass spectrometer (LC-MS) can allow for the inclusion of an internal standard and greater precision in the assessment of sample purities and decomposition.

UPLC-MS is underutilized by DPAL and is a selective and sensitive, two-step process that involves first separating compounds from a sample into individual components using UPLC then analyzing them by MS.[13] MS can identify unknown compounds by molecular weight determination (Figure 7).[19] Once a compound is injected into a MS instrument, the compound gets ionized.[19] The resulting ions are then sorted and separated by their mass-to-charge (m/z) ratios and graphed with their relative abundances.[19] This technique allows for the visualization of fragmentation patterns of the analyte that enable the identification of analyte and presence of impurities within a sample (Figure 7).[13] Due to its ability to separate compounds and their fragments by mass, UPLC-MS also offers DPAL a method of analysis using an internal standard rather than the currently used external standard and LC.

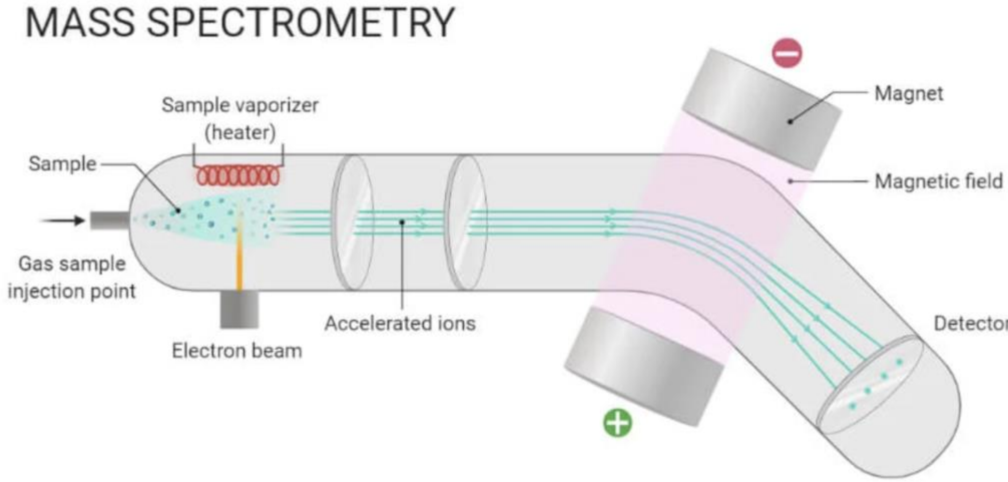

Figure 7. Depiction of mass spectrometry.[20] The compound gets ionized then sorted and separated by their m/z.

To utilize an internal standard, samples can be spiked with an isotopically labelled standard of the analyte that can help quantify the concentration of the samples present.[13] When run through the UPLC, the isotope will have the same retention time as the compound. However, when run on the MS, the known compound of the isotope will help determine the concentration of the analyte in the sample because the integration of peaks on a MS spectrum are proportional to the concentration of that constituent.[12]

Research Precedent of UPLC-MS:

The assessment of pharmaceutical decomposition is closely tied with pharmacokinetics (PK). The PK of antibiotics is particularly noteworthy due to the risk of antibiotic resistance. Even with advancements in antimicrobials, severe infections are still a leading cause of morbidity and mortality, and this problem is exacerbated when antibiotics are misused or mis-dosaged.[21] Thus, tracking therapeutic drug monitoring (TDM) is crucial in clinical facilities, such as intensive care units (ICUs). A 2018 study sought to advance TDM in ICUs by preforming HPLC-MS using samples spiked with an internal isotopic standard to quantify the antibiotic blood serum levels of patients.[21] Using this assay method, the antibiotic concentration at clinically relevant ranges in the blood was monitored and the dosage adjusted accordingly, depending on the susceptibility of the pathogen.[21] Furthermore, this technique enabled PK data to be monitored in real time through multiple blood samplings.

A 2019 study recognized that children, particularly neonates, in hospitals require varied dosages of antibiotics and antimicrobials due to the physiological changes associated with their growth and maturation.[22] Given the relationship of PK-pharmacodynamics (PK-PD) and antibiotics, and that antimicrobials are highly dependent on the nature of the drug; the microbe it targets; and the localization of infection, it is crucial to ensure that children are receiving appropriate dosages of pharmaceuticals to safely and effectively prevent both microbe proliferation and antibiotic resistance.[22] The authors of this study were able to run UPLC-MS on small samples of blood serum spiked with internal standards among patients receiving antibiotics, such as amoxicillin.[22] This method was competent in providing a simple method for the processing of patient drug levels. [22] Additionally, UPLC-MS proved well adapted to analyze batches of PK study samples containing multiple antibiotics with accuracy and precision.

Current Study's Contribution to DPAL:

Amoxicillin is one of the most commonly prescribed antibiotics for treating infections of a wide range: ear (otitis media), tonsils (tonsilitis and tonsillopharyngitis), larynx (laryngitis), lungs (pneumonia), urinary tract (UTI), and skin (gonorrhea).[23] Amoxicillin is an oral pharmaceutical and is most effective in a "time-dependent" manner, which requires a pathogen to be exposed to the antibiotic over a certain duration for successful treatment.[23] Such antibiotics are thus targeted for falsification in LMICs, which has severe impacts on global health, economy, and socioeconomics. Given this, we sought to develop an assay technique for amoxicillin using UPLC in tandem with MS and a deuterated amoxicillin (amoxicillin-d4) (Figure 8).

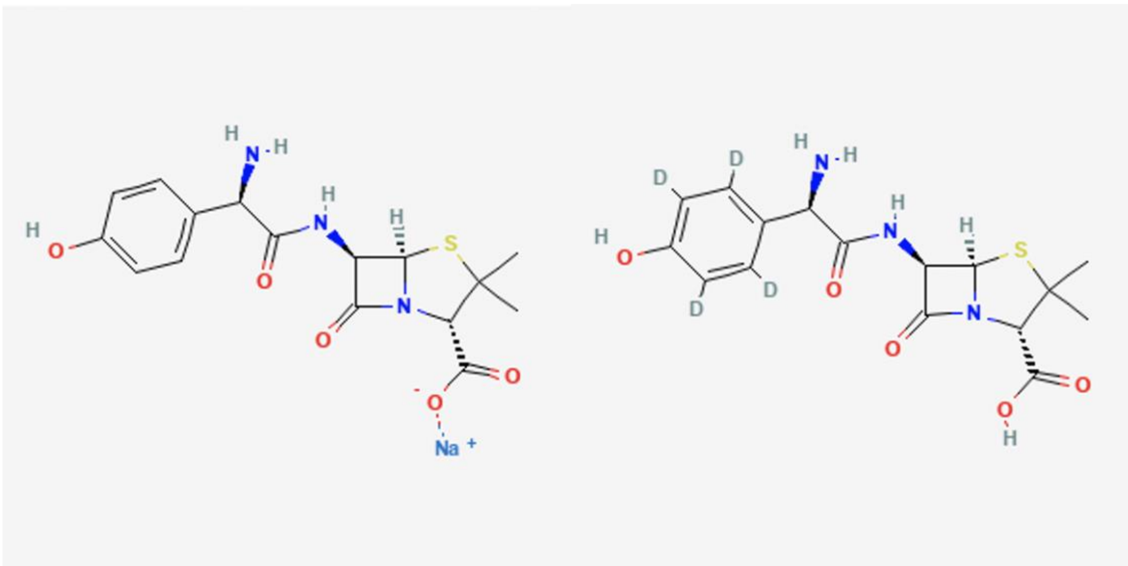

Figure 8. Chemical structures of amoxicillin (left) and amoxicillin-d4 (right).[24,25] Four hydrogen molecules have been replaced with deuterium, which results in an increased amoxicillin-d4 molar mass relative to that of amoxicillin.

In this study, we introduce UPLC-MS as a technique for identifying SF drugs within the DPAL collaboration. By spiking samples with an isotopically labelled amoxicillin and utilizing UPLC-MS, we can determine the safety of samples from DPAL partners. The current study proposes methodology for 1) obtaining and challenging a calibration curve and 2) analyzing decomposition and matrix effects of encapsulated amoxicillin that may weaken UPLC-MS signals. The utilization of UPLC-MS in the DPAL SOP would no longer limit DPAL to UV-active medicines nor require runs of external standards. UPLC-MS assays should have less noise and drift than UPLC assays and provide more thorough analyses of samples from DPAL partners in Kenya, Uganda, Tanzania, India, Nepal, or Malawi.

Materials and Methods

Materials

Liquid chromatography–mass spectrometry (LCMS)-grade solvents and water were purchased from Fischer Scientific; formic acid and amoxicillin trihydrate (Pharmaceutical Secondary Standard; Certified Reference Material) were purchased from Sigma-Aldrich. Deuterated amoxicillin-d4 was purchased from Toronto Research Chemicals, Inc. (catalog #A634238). Milli-Q water for sample preparation and glassware washing was obtained from a QPAK® 2 purification system with total organic carbon levels less than 20 ppb purchased from Millipore Sigma.

Liquid chromatography (LC) was performed using a Waters ACQUITY premier HSS T3 1.8-µm VanGuard FIT 2.1 x 150 mm column (SKU: 186009470). This H Class pump is compatible with 100% aqueous mobile phase and can be used to separate polar from non-polar compounds.[26]

LCMS spectra were obtained using a high-performance, Waters Xevo® G2-XS QTof Quadrupole Time-of-Flight Mass Spectrometer equipped with an air-cooled turbomolecular pump and a thermally controlled vacuum system that shows structural information and atomic makeup.

The LC's mobile phase was a mixture of (A) LC-MS-grade water in 0.1% formic acid (FA) and (B) acetonitrile (MeCN) in 0.1% FA. The organic solvent B inhibits bacterial growth, and the solvent was replaced every 2 weeks. Initial method conditions were 100% (A) and 0% (B); after 3 minutes, the composition was ramped to 70% (A) and 30% (B) for 2:10 minutes, then returned to initial conditions. The flow rate was 0.300 mL/min for the entire 5:10 minute duration. The temperature of the LC was set to 10 ºC; the autosampler vial compartment was also chilled to 10 °C to minimize amoxicillin degradation.

The mass spectral data was acquired via MS and positive ion modes (ESI+) using a 3.00-kV capillary voltage, 40-kV sampling cone, 80-kV source offset, 100 ºC source temperature, 37 ºC desolvation temperature, 50 L/h cone gas flow, 600 L/h, and 50-1750 Da mass range. The sample infusion flow rate was 5.0-µL/min, and fill volume was 250 µL. The LockSpray infusion flow rate was 10 µL/min, and the LockSpray Capillary voltage was 3.00 kV. The LockSpray, used for the calibration of electrospray ionization of samples, consisted of 1ug/mL Leucine enkephalin (Leu-Eu) in 1:1 acetonitrile/water (MeCN/HO) with 0.1% formic acid (FA).

The Lockspray was infused 5 mL/min. A Detector Check was run once a week, while the Lock-Mass Check was run prior to each instrumentation session. It was verified that the Leu-En signal was present at 556 m/z before proceeding to switching the sprayer from the LockSpray position to the Sample position. The LockSpray Capillary (LC) pump was primed for 5 minutes. The sample manager was then primed with wash solvent for 45 seconds. Loading the Inlet Method turned on the PDA lamp and started the LC pump at initial conditions. Once equilibrated, the samples were run. All test samples had an injection volume of 10 µL, and three replicates were run for each sample. Due to the ESI+ setting, experimental integrations at 366.10454 and 370.1296 m/z were recorded for API amoxicillin and deuterated amoxicillin-d4, respectively, (molar mass + 1H). Data were acquired using MassLynx V4.1 software. Spectra were integrated with a 0.05 Da window without smoothing.

Storage

API amoxicillin with 86% purity was stored at –20 ºC freezer, and amoxicillin capsules were stored at 4 ºC.[15] To store deuterated amoxicillin, 1.023 mg of amoxicillin-d4 with 93.81% purity was aliquoted into 100 x 10-mL centrifuge tubes. Half were stored at -20 °C and the remaining 50 tubes were placed in a –80 °C freezer for long-term storage. The Leucine enkephalin (Leu-Eu) LockSpray was stored in a 8 °C fridge; all other LCMS-grade solvents were stored at room temperature (21 °C).[27]

Thawing of Materials

Deuterated amoxicillin-d4 was thawed at room temperature for 1.5 hours then vortexed for 3 minutes. API was warmed to room temperature for 15 minutes prior to use.

Calibrating the Curve

To calibrate the curve, a mother solution and 9 dilution solutions were prepared with 229.15, 137.49, 91.66, 45.83, 22.915, 9.166, 4.58, and 0.92 ng/mL API concentrations and 80 ng/mL amoxicillin-d4 concentration.

To make the mother solution, 11.628 mg of API amoxicillin with 86% purity was measured, diluted to 100 mL in a volumetric flask using Milli-Q water, mixed for 10 minutes, then stored in a sealed media bottle. This 0.100 mg/mL mother solution was then used to make solutions 1, 2, and 9 (Table 1-M).

In separate, 2-mL LCMS vials, 0.9166 mL of each API solution and 83.4 µL of deuterated amoxicillin-d4 were combined and inverted 5 times then transferred into a clean LCMS vial through a 0.2- µL filtered syringe.

The solutions were loaded onto the temperature-controlled LC-MS autosampler carriage (10 °C) with a 10 µL injection volume, which was determined by comparing the relative standard deviations (RSD) of peak volumes resulting from 5, 7.5, and 10 µL injection volume.

For each solution, the average integral of the three replicates was used to calibrate the curve. To calculate the amoxicillin-d4 concentration, $\frac{Integration\ of\ API\ Amoxicillin}{Integration\ of\ Amoxicillin-d4}$ was plotted against $\frac{Expected\ [API\ Amoxicillin]}{Expected\ [Amoxicillin-d4]}$. The slope of the curve yielded the retention factor, and the experimental ratio was multiplied by this factor to obtain the calibration curve.

Table 1-M. Solution preparation details.

Mother		
Desired Concentration	100000	ng/mL
Volumetric Flask Size	100	mL
Amount of amoxicillin	11.628	mg
Solution 1		
Desired Concentration	183.32	ng/mL
Volumetric Flask Size	100	mL
Amount of soln M	0.200	mL
Solution 2		
Desired Concentration	137.49	ng/mL
Volumetric Flask Size	100	mL
Amount of soln M	0.150	mL
Solution 3		
Desired Concentration	91.66	ng/mL
Volumetric Flask Size	25	mL
Amount of soln 2	16.667	mL
Solution 4		
Desired Concentration	45.83	ng/mL
Volumetric Flask Size	25	mL
Amount of soln 3	12.50	mL

Solution 5		
Desired Concentration	22.915	ng/mL
Volumetric Flask Size	25	mL
Amount of soln 4	12.50	mL
Solution 6		
Desired Concentration	9.166	ng/mL
Volumetric Flask Size	25	mL
Amount of soln 3	2.50	mL
Solution 7		
Desired Concentration	4.583	ng/mL
Volumetric Flask Size	25	mL
Amount of soln 5	5.0	mL
Solution 8		
Desired Concentration	0.9166	ng/mL
Volumetric Flask Size	25	mL
Amount of soln 7	5	mL
Solution 9		
Desired Concentration	229.15	ng/mL
Volumetric Flask Size	50	mL
Amount of soln M	0.125	mL

Challenging the Curve

Two sets of the 9 solutions were prepared simultaneously using the methods described under "*Calibrating the Curve*"; one set of solutions was used to calibrate the curve and the other to challenge the curve. Once the curve was calibrated, the experimental amoxicillin concentration was calculated by:

$$\frac{Integration\ of\ API\ Amoxicillin}{Integration\ of\ Amoxicillin-d4} \times Expected\ [Amoxicillin - d4] \times\ Retention\ Factor.$$

The percent errors between the experimental and expected amoxicillin concentrations were then calculated to test the accuracy of the calibration curve.

Spiking the Curve

A capsule was stressed at 37 °C for 1 hour then its percentage of amoxicillin was calculated using DPAL's methodology: the capsule was weighed, its contents were removed using a stream of air to blow out any remaining powder, then the empty capsule was weighed.[18] The percentage of amoxicillin in a capsule was calculated by: $\frac{Mass\ of\ capsule-Mass\ of\ emptied\ capsule}{Dosage\ of\ API} \times 100.$

Three mother solutions were made: calibration curve, non-spiked, and spiked. The calibration curve mother was used to prepare the 9 solutions as described under "*Calibrating the Curve.*" The non-spiked mother also had a concentration of 0.100 mg/mL but contained only the amoxicillin capsule contents. The spiked mother also had 0.100 mg/mL encapsulated amoxicillin in addition to a 30% spike of API amoxicillin. Considering the purity of API amoxicillin, a 30% spike required the addition of 3.4883 mg of API amoxicillin to the spiked mother. Only the 137.49 ng/mL solution was made from the overdosed and spiked mothers due to its lowest RSD from *Challenging the Curve* (Table 5-A).

The expected difference in amoxicillin concentration difference between the non-spiked and spiked was calculated, where a = Experimental spiked [Amox] and b = Experimental non-spiked [Amox]: $\frac{|A-B|}{\frac{(A+B)}{2}}\ x\ 100.$

Since the non-spiked sample had a concentration of 137.49 ng/mL, the 30% spike was calculated to increase the amoxicillin concentration by 41.247 ng/mL. Then the percent error between the expected and experimental amoxicillin concentrations in spiked and non-spiked solutions was determined.

Number of theoretical plates (N) was calculated using DPAL's SOP equation: $5.54\ x\ \frac{Retention\ Time}{Peak\ Width\ at\ Half\ the\ Height}$. The tailing factor (T) was also determined using DPAL's SOP (Figure 1-M): $\frac{a+b}{2a}$.

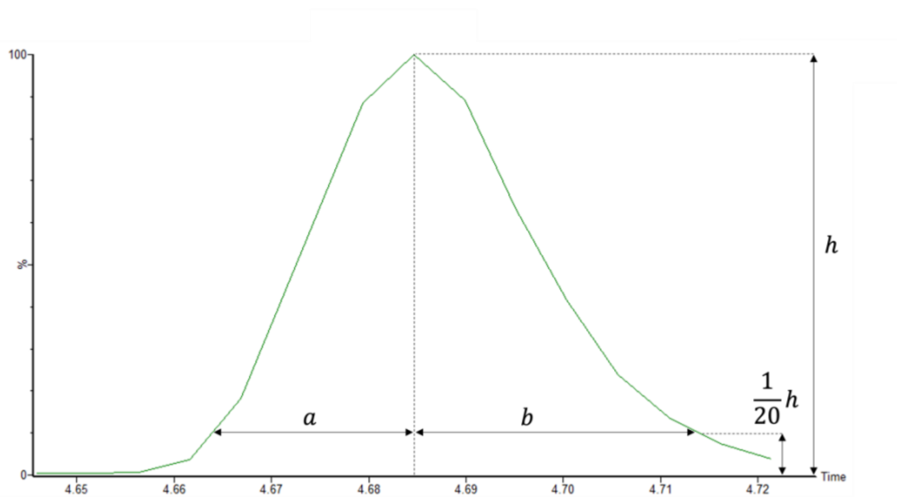

Figure 1-M. Diagram depicting measurements for calculating T. The a and b values were evaluated at 10%.

Results & Discussions

Determining the Injection Volume

To determine the injection volume of amoxicillin (referred to as amox in tables and figures) samples, 6 replicate injections were run using 5, 7.5, and 10 μL injection volumes (Table 1-A, Table 2-A, Table 3-A). The range of RSD for amoxicillin using a 5, 7.5, or 10 μL injection volume was 1.23-53.95, 0.88-30.33, and 1.02-17.90 respectively. The range of RSD for amoxicillin-d4 using a 5, 7.5, or 10 μL injection volume was 1.38-6.51, 1.53-3.42, and 0.84-3.85 respectively. The injection volume of 10 μL was preferred due to its low RSD for amoxicillin and its relatively low amoxicillin-d4 RSD.

Calibration Curve

The integrals of amoxicillin and amoxicillin-d4 in samples of 229.15, 137.49, 91.66, 45.83, 22.915, 9.166, 4.58, and 0.92 ng/mL concentration were taken; amoxicillin peak integrals decreased as the concentration decreased, while amoxicillin-d4 peak integrals were relatively consistent across solutions (Table 4-A). The $\frac{Integration\ of\ Amoxicillin}{Integration\ of\ Amoxicillin-d4}$ was plotted against $\frac{Expected\ [Amoxicillin]}{Expected\ [Amoxicillin-d4]}$ and the line of best fit yielded the retention factor (referred to as RF in tables and figures) (Figure 1-R.A, Table 4-A). The retention factor, 0.306, was then used to obtain the calibration curve (Figure 1-R.B).

The precision of this method to obtain the calibration curve was demonstrated by low RSD (Table 4-A). When calibrating the curve, the RSD of amoxicillin and amoxicillin-d4 integrals ranged 0.33-5.78 and 0.58-5.08, respectively (Table 4-A). Further, the slope of the calibration curve; R^2 value; and the fact that each point represents three replicates are all indications of the curve's high accuracy (Figure 1-R.B).

Challenging the Calibration Curve

The percent error between the calibration curve and the challenger ranged from 0.25% to 2.97%, corresponding with the 137.49 ng/mL and 9.166 ng/mL respectively (Table 5-A).

When challenging the curve, the RSD for amoxicillin and amoxicillin-d4 were: 0.30-1.65 and 1.02-2.20 respectively (Table 5-A). This precision was consistent across different experiments, as the RSD for amoxicillin, amoxicillin-d4, and the ratio of the two were: 0.63-4.08, 1.32-4.56, and 0.51-6.73 (Table 5-A).

Spiking the Curve

From challenging the curve, the 137.49 ng/mL solution had the lowest percent error and thus was used to test matrix effects and decomposition from the amoxicillin capsule (Table 5-A). First, a calibration curve was obtained (Table 6-A, Figure 1-A). Next, this calibration curve was used to determine the amoxicillin concentration in the spiked and non-spiked solutions. The spiked and non-spiked solutions had concentrations ranging from 145-148 and 97.6-99.1 ng/mL, respectively (Table 7-A). The percent error between the spiked and non-spiked solutions ranged from 0.197-5.56% (Table 7-A).

Using a calibration curve, the amount of amoxicillin in a solution that was prepared to be 137.49 ng/mL was calculated to be 97.89 ng/mL. This concentration indicates that the encapsulated amoxicillin underwent decomposition while being stressed. Whereas the low percent error between the amoxicillin concentration in the spiked and non-spiked solutions suggest that matrix effects using this methodology are low for amoxicillin capsules.

The theoretical plates (N) and tailing factor (T) were calculated on the non-spiked and spiked spectra. The N values for the non-spiked amoxicillin-d4 and amoxicillin were 123326 and

125724; the T values were 1.4567 and 1.3311, respectively (Figure 2-R). The N values for the spiked amoxicillin-d4 and amoxicillin were 129586 and 157004; the T values were 1.2091 and 1.3839, respectively (Figure 2-R).

The high N values indicate that our column was highly efficient and had a considerable separation power. Whereas the T values indicate the leading tails of the curves were longer than the trailing tails. The T values are consistent with that of DPAL's SOP that commonly recommends a trailing factor of less than 2.0.[18]

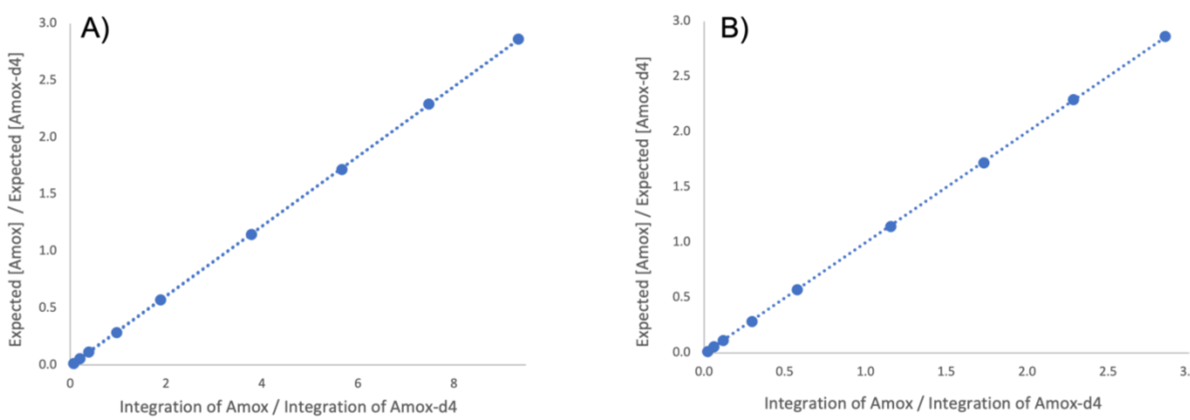

Figure 1-R. A) Linear line of best fit to determine the retention factor ($y = 0.306x$, $R^2 = 1$). **B)** The calibration curve with a linear line of best fit ($y = 1.00x$, $R^2 = 1$). Each point on **A** and **B** represents three replicates.

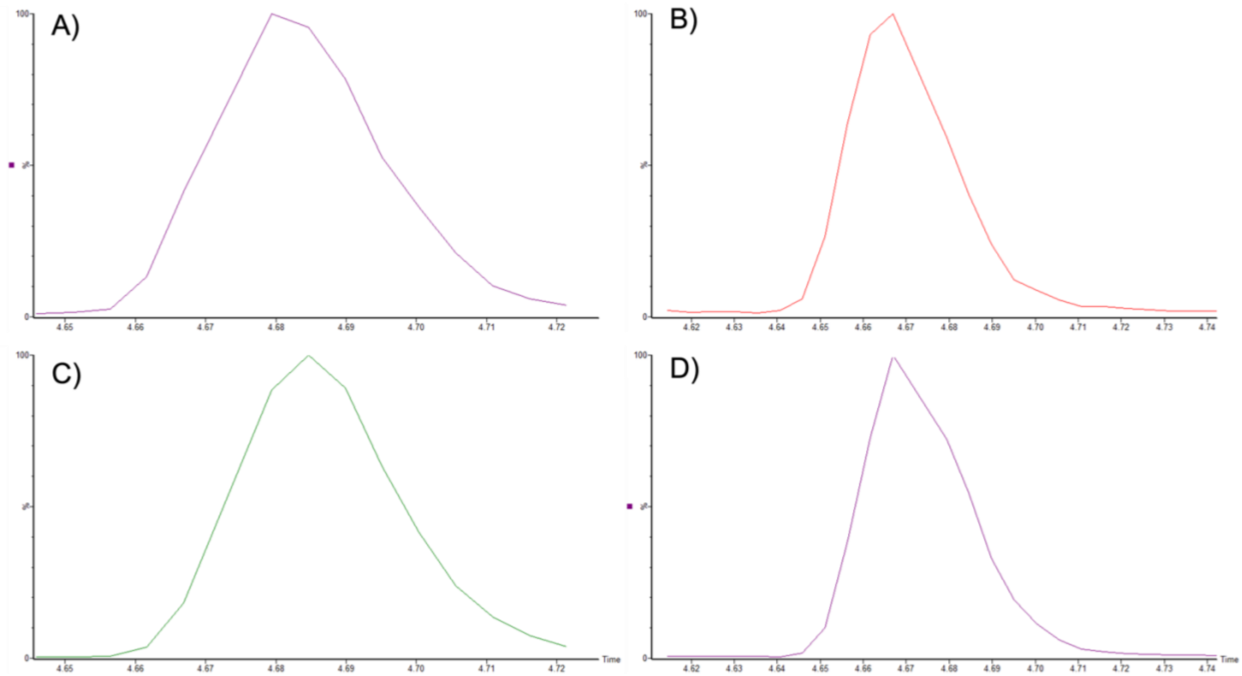

Figure 2-R. Spectra of spiked and non-spiked solutions. **A)** Non-spiked amoxicillin-d4, with retention time 4.67 min; N = 123326; T = 1.4567 **B)** Spiked amoxicillin-d4, with retention time 4.68 min; N = 129586; T = 1.2091 **C)** non-spiked amoxicillin, with retention time 4.67 min; N = 125724; T = 1.3311 and **D)** spiked amoxicillin, with retention time 4.68 min; N = 157004; T = 1.3839.

Conclusions

This project sought to develop a methodology for analyzing amoxicillin samples using ultra performance liquid chromatography in tandem with mass spectrometry for DPAL.

An accurate and precise injection volume was successfully determined for obtaining a calibration curve. Three replicates of nine solutions were sufficient for obtaining a retention factor that yielded an accurate and precise calibration curve with a slope and R^2 value of 1. When the calibration curve was challenged, the RSD between expected and experimental amoxicillin and amoxicillin-d4 were less than 3%, which reinforces the exactitude of the curve. The calibration curve and a spiked solution were used to analyze decomposition and matrix effects of encapsulated amoxicillin. After undergoing one hour of stress, the encapsulated amoxicillin decomposed, but its matrix effects on UPLC-MS were minimal as reflected by the low percent error between expected and experimental amoxicillin concentrations in the spiked and non-spiked samples.

The methodology presented here allows DPAL to utilize UPLC-MS to analyze amoxicillin samples. This would no longer limit DPAL to UV-active medicines nor require runs of external standards. Further, this methodology can be extracted for analysis of other pharmaceuticals for DPAL and its partners.

Acknowledgements

I would like to thank Dr. Anna Wenzel for her never-ending, nurturing, and expert advice over the past five years. From *Drug Development, Policy & Innovation* to *Organic Chemistry* to Zoom-meetings-throughout-COVID, you have remained steadfast in helping me achieve academic success and personal growth. It is incredible to reflect on how long I have known you; when we first met in the fall of 2017 you were pregnant with Maddie and Emily. You are truly an inspiration for how I should live and learn; you are a role model for your strength, knowledge, and compassion. You were willing to take me, a biology major, to independently carry out your DPAL project; it has been an honor to do so, even with all the hiccups The Diva makes for us. Thank you for everything you have taught me during my time at Pitzer College.

I would also like to thank Dr. Ethan Van Arnam and Kyle McCarthy for their exceeding knowledge of the LCMS. Without you both, this project would not have been possible.

References

(1) United States Pharmacopeia. Combatting Substandard and Falsified Medicines Policy Position. *United States Pharmacopeia*.

(2) World Health Organization. *A study on the public health and socioeconomic impact of substandard and falsified medical products*; World Health Organization: Geneva, 2017.

(3) Ghanem, N. *Substandard and falsified medicines: global and local efforts to address a growing problem* https://pharmaceutical-journal.com/article/research/substandard-and-falsified-medicines-global-and-local-efforts-to-address-a-growing-problem (accessed 2021 -10-06).

(4) Funestrand, H.; Liu, R.; Lundin, S.; Troein, M. Substandard and Falsified Medical Products Are a Global Public Health Threat. A Pilot Survey of Awareness among Physicians in Sweden. *J Public Health (Oxf)* **2019**, *41* (1), e95–e102. https://doi.org/10.1093/pubmed/fdy092.

(5) Buckley, G. J.; Gostin, L. O.; Committee on Understanding the Global Public Health Implications of Substandard, F.; Health, B. on G.; Medicine, I. of. *The Effects of Falsified and Substandard Drugs*; National Academies Press (US), 2013.

(6) Newton, P. N.; McGready, R.; Fernandez, F.; Green, M. D.; Sunjio, M.; Bruneton, C.; Phanouvong, S.; Millet, P.; Whitty, C. J. M.; Talisuna, A. O.; Proux, S.; Christophel, E. M.; Malenga, G.; Singhasivanon, P.; Bojang, K.; Kaur, H.; Palmer, K.; Day, N. P. J.; Greenwood, B. M.; Nosten, F.; White, N. J. Manslaughter by Fake Artesunate in Asia—Will Africa Be Next? *PLOS Medicine* **2006**, *3* (6), e197. https://doi.org/10.1371/journal.pmed.0030197.

(7) Questions & Answers about Counterfeit Drugs https://www.bayer.com/en/pharma/background-information-on-counterfeit-drugs (accessed 2022 -04 -23).

(8) Woodcock, J. Safeguarding Pharmaceutical Supply Chains in a Global Economy - 10/30/2019 https://www.fda.gov/news-events/congressional-testimony/safeguarding-pharmaceutical-supply-chains-global-economy-10302019 (accessed 2022 -04 -23).

(9) Ozawa, S.; Evans, D. R.; Bessias, S.; Haynie, D. G.; Yemeke, T. T.; Laing, S. K.; Herrington, J. E. Prevalence and Estimated Economic Burden of Substandard and Falsified Medicines in Low- and Middle-Income Countries: A Systematic Review and Meta-Analysis. *JAMA Network Open* **2018**, *1* (4), e181662. https://doi.org/10.1001/jamanetworkopen.2018.1662.

(10) Borse, N. N.; Cha, J.; Chase, C. G.; Gaur, R.; Koduri, C. K.; Kokai-Kun, J. F.; Kwan, D. C.; Lee, R.; Moore, J. C.; Raghavendran, V.; Takara, L. S.; Zeine, C. Responding to the Surge of Substandard and Falsified Health Products Triggered by the Covid-19 Pandemic. 11.

(11) Bliese, S. L.; Berta, M.; Lieberman, M. Involving Students in the Distributed Pharmaceutical Analysis Laboratory: A Citizen-Science Project to Evaluate Global Medicine Quality. *J. Chem. Educ.* **2020**, *97* (11), 3976–3983. https://doi.org/10.1021/acs.jchemed.0c00904.

(12) Basic Principles of HPLC, MS & LC-MS https://www.chemyx.com/support/knowledge-base/applications/basic-principles-hplc-ms-lc-ms/ (accessed 2021-10-19).

(13) Liquid Chromatography Mass Spectrometry (LC-MS) Information - US //www.thermofisher.com/us/en/home/industrial/mass-spectrometry/mass-spectrometry-learning-center/liquid-chromatography-mass-spectrometry-lc-ms-information.html (accessed 2021-10-08).

(14) Ahuja, S.; Dong, M. *Handbook of Pharmaceutical Analysis by HPLC*; Elsevier, 2005.

(15) Binson, G.; Grignon, C.; Le Moal, G.; Lazaro, P.; Lelong, J.; Roblot, F.; Venisse, N.; Dupuis, A. Overcoming Stability Challenges during Continuous Intravenous Administration of High-Dose Amoxicillin Using Portable Elastomeric Pumps. *PLoS One* **2019**, *14* (8), e0221391. https://doi.org/10.1371/journal.pone.0221391.
(16) Aryal, S. HPLC- Definition, Principle, Parts, Types, Uses, Diagram https://microbenotes.com/high-performance-liquid-chromatography-hplc/ (accessed 2022 -04 -23).
(17) Dyad Labs. HPLC vs. UPLC. Dyad Labs https://dyadlabs.com/hplc-vs-uplc (accessed 2021-10-09)
(18) Lieberman, M. HPLC Methodology Manual. *University of Notre Dame.* Revised 2020-03-05.
(19) What is Mass Spectrometry? https://www.broadinstitute.org/technology-areas/what-mass-spectrometry (accessed 2021 -10 -19).
(20) Aryal, S. Mass Spectrometry (MS)- Principle, Working, Instrumentation, Steps, Applications https://microbenotes.com/mass-spectrometry-ms-principle-working-instrumentation-steps-applications/ (accessed 2022 -04 -23).
(21) Schuster, C.; Sterz, S.; Teupser, D.; Brügel, M.; Vogeser, M.; Paal, M. Multiplex Therapeutic Drug Monitoring by Isotope-Dilution HPLC-MS/MS of Antibiotics in Critical Illnesses. *JoVE (Journal of Visualized Experiments)* **2018**, No. 138, e58148. https://doi.org/10.3791/58148.
(22) Magréault, S.; Leroux, S.; Touati, J.; Storme, T.; Jacqz-Aigrain, E. UPLC/MS/MS Assay for the Simultaneous Determination of Seven Antibiotics in Human Serum–Application to Pediatric Studies. *Journal of Pharmaceutical and Biomedical Analysis* **2019**, *174*, 256–262. https://doi.org/10.1016/j.jpba.2019.03.004.
(23) Akhavan, B. J.; Khanna, N. R.; Vijhani, P. Amoxicillin. In *StatPearls*; StatPearls Publishing: Treasure Island (FL), 2022.
(24) PubChem. Amoxicillin sodium https://pubchem.ncbi.nlm.nih.gov/compound/23663126 (accessed 2022 -04 -23).
(25) PubChem. Amoxicillin D4 https://pubchem.ncbi.nlm.nih.gov/compound/76974031 (accessed 2022 -04 -23).
(26) ACQUITY Premier HSS T3 Column with VanGuard FIT, 1.8 µm, 2.1 x 50 mm, 1/pk https://www.waters.com/nextgen/us/en/shop/columns/186009470-acquity-premier-hss-t3-column-with-vanguard-fit-18--m-21-x-50-mm.html (accessed 2022 -03 -20).
(27) Canzani, D.; Hsieh, K.; Standland, M.; Hammack, W.; Aldeek, F. UHPLC–MS/MS Method for the Quantitation of Penicillin G and Metabolites in Citrus Fruit Using Internal Standards. *Journal of Chromatography B* **2017**, *1044–1045*, 87–94. https://doi.org/10.1016/j.jchromb.2017.01.012.

Appendix

Table 1-A. Integrals of peaks for solutions with concentrations of amoxicillin and amoxicillin-d4 described in columns 1 and 2, respectively, and an injection volume of 5 μL.

Expected [Amox] (ng/mL)	Expected [Amox-d4] (ng/mL)	5 μL Injection Volume					
		Amox Peak Volume	Amox Peak Volume Average	Amox Peak Volume RSD	Amox-d4 Peak Volume	Amox-d4 Peak Volume Average	Amox-d4 Peak Volume RSD
229.15	80	11938	12061	2.1515	1282	1332	6.506
		12047			1391		
		11999			1202		
		12570			1445		
		11834			1305		
		11978			1366		
183.32		9173	9884	4.269	1272	1391	4.901
		9643			1387		
		9882			1376		
		10282			1446		
		10244			1467		
		10080			1396		
137.49		7936	7869	1.232	1397	1478	3.130
		7732			1490		
		7968			1503		
		7765			1452		
		7889			1525		
		7921			1500		
91.66		5296	5345	1.723	1496	1505	1.383
		5454			1512		
		5393			1513		
		5351			1483		
		5190			1538		
		5387			1485		
45.83		2666	2739	2.652	1464	1513	3.231
		2785			1488		
		2734			1525		
		2795			1561		
		2815			1576		
		2639			1463		
22.915		1396	1371	4.962	1496	1511	1.656
		1417			1543		
		1407			1530		
		1414			1485		
		1241			1524		
		1352			1485		
9.166		475	493	11.4	1489	1489	3.462
		530			1406		
		535			1556		
		552			1506		
		461			1518		
		405			1461		

Expected [Amox] (ng/mL)	Expected [Amox-d4] (ng/mL)	5 μL Injection Volume					
		Amox Peak Volume	Amox Peak Volume Average	Amox Peak Volume RSD	Amox-d4 Peak Volume	Amox-d4 Peak Volume Average	Amox-d4 Peak Volume RSD
4.583	80	180	226	10.8	1599	1560	2.159
		224			1587		
		225			1572		
		250			1526		
		234			1562		
		240			1514		
0.9166		26	60	54	1456	1481	2.525
		81			1507		
		36			1524		
		30			1442		
		96			1513		
		88			1445		

Table 2-A. Integrals of peaks for solutions with concentrations of amoxicillin and amoxicillin-d4 described in columns 1 and 2, respectively, and an injection volume of 7.5 µL.

Expected [Amox] (ng/mL)	Expected [Amox-d4] (ng/mL)	7.5 µL Injection Volume					
		Amox Peak Volume	Amox Peak Volume Average	Amox Peak Volume RSD	Amox-d4 Peak Volume	Amox-d4 Peak Volume Average	Amox-d4 Peak Volume RSD
229.15	80	17828	17182	2.6854	2010	2015	2.463
		16520			1991		
		17352			2056		
		16799			2032		
		17357			2070		
		17233			1933		
183.32		14373	14595	1.4748	2101	2070	1.625
		14768			2095		
		14799			2041		
		14717			2088		
		14628			2080		
		14287			2017		
137.49		11438	11230	1.7985	2240	2149	2.805
		11327			2156		
		10924			2129		
		11035			2109		
		11333			2071		
		11325			2191		
91.66		7709	7535	2.027	2135	2100	3.417
		7504			1989		
		7599			2203		
		7371			2070		
		7350			2084		
		7677			2121		
45.83		3838	3811	0.8837	2131	2125	1.531
		3825			2155		
		3849			2089		
		3778			2088		
		3764			2122		
		3813			2166		
22.915		1947	1950	1.444	2177	2137	2.461
		1933			2158		
		1921			2108		
		1929			2202		
		1978			2057		
		1990			2119		
9.166		789	771	2.01	2246	2195	2.880
		779			2127		
		756			2213		
		785			2269		
		753			2112		
		763			2203		

Expected [Amox] (ng/mL)	Expected [Amox-d4] (ng/mL)	7.5 µL Injection Volume					
		Amox Peak Volume	Amox Peak Volume Average	Amox Peak Volume RSD	Amox-d4 Peak Volume	Amox-d4 Peak Volume Average	Amox-d4 Peak Volume RSD
4.583	80	180	226	10.8	1599	1560	2.159
		224			1587		
		225			1572		
		250			1526		
		234			1562		
		240			1514		
0.9166		26	60	54	1456	1481	2.525
		81			1507		
		36			1524		
		30			1442		
		96			1513		
		88			1445		

Table 3-A. Integrals of peaks for solutions with concentrations of amoxicillin and amoxicillin-d4 described in columns 1 and 2, respectively, and an injection volume of 10 µL.

Expected [Amox] (ng/mL)	Expected [Amox-d4] (ng/mL)	10 µL Injection Volume					
		Amox Peak Volume	Amox Peak Volume Average	Amox Peak Volume RSD	Amox-d4 Peak Volume	Amox-d4 Peak Volume Average	Amox-d4 Peak Volume RSD
229.15	80	20430	20098	2.0264	2659	2575	2.838
		20455			2635		
		19379			2498		
		19890			2595		
		20174			2586		
		20258			2477		
183.32		19201	18838	2.6104	2613	2579	2.669
		19602			2522		
		18549			2517		
		18285			2683		
		18872			2616		
		18517			2522		
137.49		14038	14135	1.0174	2599	2599	0.844
		14222			2574		
		14115			2576		
		14231			2624		
		14294			2624		
		13908			2597		
91.66		9500	9336	2.297	2533	2634	2.581
		9434			2679		
		9027			2673		
		9110			2568		
		9542			2704		
		9403			2644		
45.83		4625	4751	1.777	2746	2648	3.020
		4737			2564		
		4807			2604		
		4730			2675		
		4876			2570		
		4732			2729		
22.915		2503	2438	3.209	2494	2614	2.908
		2331			2631		
		2452			2690		
		2498			2577		
		2348			2696		
		2493			2596		
9.166		897	950	4.14	2737	2690	3.421
		957			2557		
		933			2796		
		932			2770		
		1013			2644		
		967			2638		

Expected [Amox] (ng/mL)	Expected [Amox-d4] (ng/mL)	10 µL Injection Volume					
		Amox Peak Volume	Amox Peak Volume Average	Amox Peak Volume RSD	Amox-d4 Peak Volume	Amox-d4 Peak Volume Average	Amox-d4 Peak Volume RSD
4.583	80	490	453	9.76	2567	2519	2.376
		372			2550		
		466			2426		
		444			2570		
		493			2463		
		454			2535		
0.9166		146	120	18.2	2264	2205	3.854
		86			2213		
		134			2143		
		137			2274		
		112			2271		
		116			2065		

Table 4-A. Integrals of peaks for solutions with concentrations of amoxicillin and amoxicillin-d4 described in columns 1 and 2, respectively, to obtain the retention factor.

Expected [Amox] (ng/mL)	Expected [Amox-d4] (ng/mL)	Amox Peak Volume	Amox Peak Volume Average	Amox Peak Volume RSD	Amox-d4 Peak Volume	Amox-d4 Peak Volume Average	Amox-d4 Peak Volume RSD	Amox Peak Volume / Amox-d4 Peak Volume	Expected [Amox] / Expected [Amox-d4]
229.15	80	20194	20211	0.33217	2166	2164	0.6519	9.340	2.8644
		20154			2149				
		20285			2177				
183.32		15140	16203	5.7760	2040	2167	5.084	7.478	2.2915
		16564			2220				
		16904			2240				
137.49		12772	12878	2.7679	2262	2273	3.325	5.666	1.7186
		12586			2203				
		13275			2353				
91.66		8572	8365	4.671	2248	2211	2.977	3.783	1.146
		8608			2250				
		7914			2135				
45.83		4277	4229	1.253	2264	2243	0.9365	1.885	0.5729
		4237			2244				
		4172			2222				
22.915		2240	2224	1.169	2303	2288	0.5819	0.9719	0.28644
		2194			2285				
		2238			2277				
9.166		895	871	2.70	2241	2268	1.088	0.384	0.1146
		848			2275				
		871			2289				
4.583		467	458	2.36	2299	2266	1.935	0.202	0.0573
		461			2216				
		446			2282				
0.9166		165	165	0.351	2271	2280	0.6713	0.072	0.0115
		164			2298				
		165			2272				

Table 5-A. Integrals of peaks for solutions with concentrations of amoxicillin and amoxicillin-d4 described in columns 1 and 2, respectively, to challenge the calibration curve.

Expected [Amox] (ng/mL)	Expected [Amox-d4] (ng/mL)	Amox Peak Volume	Amox Peak Volume Average	Amox-d4 Peak Volume	Amox-d4 Peak Volume Average	Amox Peak Volume / Amox-d4 Peak Volume	RF	Experimental [Amox] (ng/mL)	% Error
229.15	80	19637	19841	2130	2108	9.411	0.306	230	0.402
		19986		2087					
		19899		2108					
183.32		16518	16649	2123	2178	7.645		187	1.96
		16964		2212					
		16465		2198					
137.49		12317	12257	2208	2185	5.609		137	0.255
		12373		2204					
		12080		2143					
91.66		8114	8133	2226	2206	3.686		90.1	1.68
		8160		2213					
		8124		2180					
45.83		3961	4015	2192	2204	1.822		44.5	2.80
		4043		2179					
		4042		2240					
9.166		859	864	2239	2238	0.386		9.44	2.97
		862		2203					
		871		2272					

Table 6-A. Integrals of peaks for solutions with concentrations of amoxicillin and amoxicillin-d4 described in columns 1 and 2, respectively, to obtain the calibration curve while analyzing decomposition and matrix effects of encapsulated amoxicillin.

Expected [Amox] (ng/mL)	Expected [Amox-d4] (ng/mL)	Amox Peak Volume	Amox Peak Volume Average	Amox Peak Volume RSD	Amox-d4 Peak Volume	Amox-d4 Peak Volume Average	Amox-d4 Peak Volume RSD	Amox Peak Volume / Amox-d4 Peak Volume	Expected [Amox] / Expected [Amox-d4]
229.15	80	20457	20095	3.1374	2223	2184	2.706	9.201	2.8644
		19367			2116				
		20461			2213				
183.32		16882	17625	3.6554	2255	2380	4.562	7.405	2.2915
		18023			2440				
		17971			2446				
137.49		13943	13648	2.7799	2437	2431	2.702	5.613	1.7186
		13781			2494				
		13220			2363				
91.66		9575	9594	3.689	2485	2503	2.692	3.832	1.1458
		9957			2578				
		9250			2447				
45.83		4511	4479	0.6292	2470	2453	1.320	1.826	0.5729
		4470			2416				
		4457			2474				

Expected [Amox] (ng/mL)	Expected [Amox-d4] (ng/mL)	Amox Peak Volume	Amox Peak Volume Average	Amox Peak Volume RSD	Amox-d4 Peak Volume	Amox-d4 Peak Volume Average	Amox-d4 Peak Volume RSD	Amox Peak Volume / Amox-d4 Peak Volume	Expected [Amox] / Expected [Amox-d4]
22.915	80	2425	2407	0.6627	2494	2451	1.843	0.9818	0.2864
		2399			2404				
		2396			2456				
9.166		992	994	2.17	2398	2438	3.780	0.408	0.1146
		1016			2543				
		973			2372				
4.583		511	521	4.08	2388	2304	3.305	0.226	0.0573
		506			2283				
		545			2240				

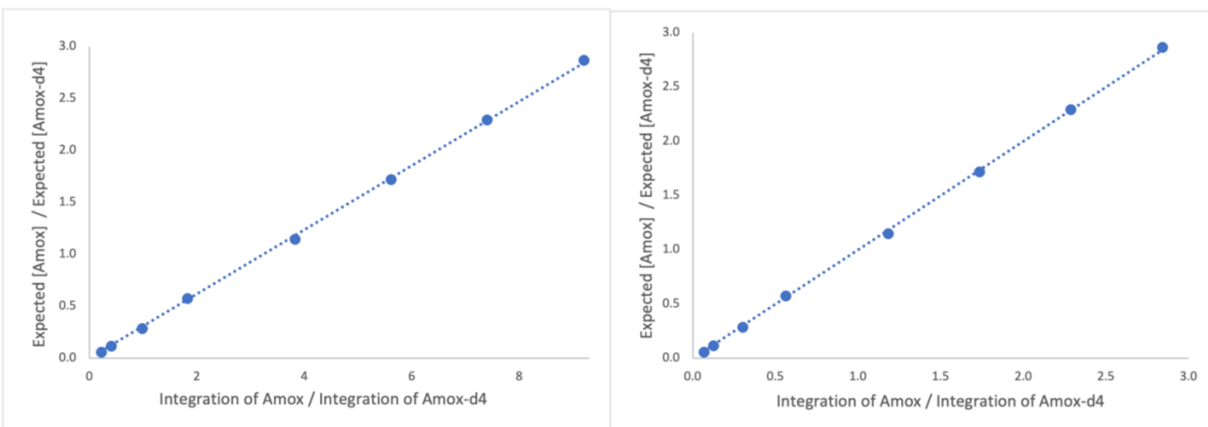

Figure 1-A. Calibration curve while analyzing decomposition and matrix effects of encapsulated amoxicillin. **A)** Linear line of best fit to determine the retention factor ($y = 0.309x$, $R^2 = 1$). **B)** The calibration curve with a linear line of best fit ($y = 1.000x$, $R^2 = 1$). Each point on **A** and **B** represents three replicates.

Table 7-A. Integrals of peaks for solutions with concentrations of amoxicillin and amoxicillin-d4 described in columns 2 and 3, respectively, to analyze decomposition and matrix effects of encapsulated amoxicillin.

<table>
<tr><th></th><th>Expected [Amox] (ng/mL)</th><th>Expected [Amox-d4] (ng/mL)</th><th>Amox Peak Volume</th><th>Amox Peak Volume Average</th><th>Amox-d4 Peak Volume</th><th>Amox-d4 Peak Volume Average</th><th>Amox Peak Volume / Amox-d4 Peak Volume</th><th>RF</th><th>Experimental [Amox]</th><th>Experimental [Amox] Difference Between Spiked and Non-Spiked</th><th>Expected [Amox] Difference Between Spiked and Non-Spiked</th><th>% Error</th></tr>
<tr><td rowspan="3">Non-spiked</td><td rowspan="3">137.49</td><td rowspan="6">80</td><td>8767</td><td rowspan="3">8930</td><td>2220</td><td rowspan="3">2254</td><td>3.949</td><td rowspan="6">0.309</td><td>97.6</td><td>41.3</td><td rowspan="3">41.247</td><td>0.197</td></tr>
<tr><td>8984</td><td>2241</td><td>4.009</td><td>99.1</td><td>39.0</td><td>5.56</td></tr>
<tr><td>9038</td><td>2302</td><td>3.926</td><td>97.0</td><td>39.9</td><td>3.28</td></tr>
<tr><td rowspan="3">Spiked</td><td rowspan="3">178.737</td><td>13358</td><td rowspan="3">13430</td><td>2224</td><td rowspan="3">2259</td><td>6.006</td><td>148</td><td>41.3</td><td rowspan="3" colspan="2"></td></tr>
<tr><td>13538</td><td>2276</td><td>5.948</td><td>147</td><td>40.4</td></tr>
<tr><td>13395</td><td>2277</td><td>5.883</td><td>145</td><td>39.3</td></tr>
</table>